JOURNAL OF ENVIRONMENTAL SCIENCES 70 (2018) 37–44

Available online at www.sciencedirect.com

ScienceDirect

www.elsevier.com/locate/jes

JES JOURNAL OF ENVIRONMENTAL SCIENCES

www.jesc.ac.cn

Thermal internal boundary layer and its effects on air pollutants during summer in a coastal city in North China

Jie Wei[1,3], *Guiqian Tang*[1,2,*], *Xiaowan Zhu*[1,3], *Lili Wang*[1], *Zirui Liu*[1], *Mengtian Cheng*[1], *Christoph Münkel*[4], *Xin Li*[1,5], *Yuesi Wang*[1,2]

1. *State Key Laboratory of Atmospheric Boundary Layer Physics and Atmospheric Chemistry (LAPC), Institute of Atmospheric Physics, Chinese Academy of Sciences, Beijing 100029, China*
2. *Center for Excellence in Regional Atmospheric Environment, Institute of Urban Environment, Chinese Academy of Sciences, Xiamen 361021, China*
3. *University of Chinese Academy of Sciences, Beijing 100049, China*
4. *Vaisala GmbH, 22607 Hamburg, Germany*
5. *Beijing Municipal Committee of China Association for Promoting Democracy, Beijing 100035, China*

ARTICLE INFO

Article history:
Received 7 July 2017
Revised 14 October 2017
Accepted 8 November 2017
Available online 12 November 2017

Keywords:
Thermal internal boundary layer
Ceilometer
Air pollutants
Sea breeze

ABSTRACT

The thermal internal boundary layer (TIBL) is associated with coastal pollution dispersion, which can result in high concentrations of air pollutants near the surface of the Earth. In this study, boundary layer height data which were obtained using a ceilometer were used to assess the effect of the TIBL on atmospheric pollutants in Qinhuangdao, a coastal city in North China. A TIBL formed on 33% of summer days. When a TIBL formed, the sunshine duration was 2.4 hr longer, the wind speed was higher, the wind direction reflected a typical sea breeze, and the boundary layer height was lower from 9:00 LT to 20:00 LT compared to days without a TIBL. If no TIBL formed, the average concentrations of $PM_{2.5}$ and PM_{10} decreased with increasing boundary layer height. However, when a TIBL was observed, the average concentrations of $PM_{2.5}$ and PM_{10} increased with increasing boundary layer height. Because the air from the sea is clean, $PM_{2.5}$ and PM_{10} concentrations reached minimums in the daytime at 16:00 LT. After 16:00 LT, the $PM_{2.5}$ and PM_{10} concentrations increased rapidly on days when a TIBL formed, which indicated that the TIBL leads to the rapid accumulation of atmospheric pollutants in the evening. Therefore, the maximum concentrations of particulate matters were larger when a TIBL formed compared to when no TIBL was present during the night. These results indicate that it is suitable for outdoor activities in the daytime on days with a TIBL in coastal cities.

Introduction

The atmospheric boundary layer is the lowest atmospheric layer, located 1 to 2 km above the surface of Earth. This is the main layer where human activities take place, and the emission, transmission and transformation of pollutants occur in this layer. Therefore, the environmental problems within the atmospheric boundary layer directly influence the survival and health of human beings (Tang et al., 2017a).

The height of the atmospheric boundary layer can be defined as the height at which the turbulent momentum flux and heat flux caused by the ground both decrease to minimum values (such as 1% of the surface value) (Stull, 1988). The height of the atmospheric boundary layer is an important parameter that

* *Corresponding author. E-mail:* tgq@dq.cern.ac.cn (Guiqian Tang).

https://doi.org/10.1016/j.jes.2017.11.006
1001-0742/

influences the diffusion of air pollutants, and an important physical quantity that reflects the convection and diffusion characteristics of vertical atmospheric circulation. Multiple approaches have been used to measure the height of the atmospheric boundary layer, and these approaches have been summarized in previous studies (Beyrich, 1997; Emeis et al., 2008; Seibert et al., 2000). Recently, light detection and ranging (LIDAR) has experienced rapid development, and numerous studies have used LIDAR to detect the height of the atmospheric boundary layer (Scarino et al., 2014; White et al., 2010; Wiegner et al., 2006). Additionally, an eye-safe ceilometer has been developed that uses near-infrared band lasers to detect the height of the boundary layer. Due to its low cost, easy accessibility and consecutive detection ability, ceilometer detection has become the optimal method for the detection of the atmospheric boundary layer height (Emeis and Schäfer, 2006; Tang et al., 2015, 2016; Zhu et al., 2016).

In coastal regions, the formation of a thermal internal boundary layer (TIBL) is a common boundary layer phenomenon. In the sunny daytime, the sea breeze will blow the stable or neutrally stratified air over the sea towards land. The surface heating effect and dynamic disturbance effect intensify the turbulence in the lowest atmospheric layer to form an unstable layer, which develops into the TIBL. Notably, the TIBL progressively grows from the coastline to inland areas. Garratt (1990) systematically summarized the TIBL. Sicard et al. (2006) utilized elastic-backscatter LIDAR to measure the boundary layer height in the coastal city Barcelona. They found that the relatively low boundary layer height is related to the mesoscale compensatory subsidence over the sea and TIBL formation in summer. Prabha et al. (2002) studied the influence of changing synoptic scale conditions on the turbulent characteristics of the TIBL using a mini-sonic detection and ranging (SODAR) system, and concluded that the TIBL characteristics over the coastal land after the onset of the sea breeze are similar to those of the shallow convective boundary layer commonly observed over plain areas. Therefore, the height of the TIBL can be considered the height of the shallow convective boundary layer.

Several methods can be used to estimate the height of the TIBL. Using the results of a large eddy simulation, Calmet and Mestayer (2016) noted that the inversion height may indicate the top of the TIBL, and the TIBL depth may be determined by three methods, including from potential temperature profiles, heat flux profiles or turbulent kinetic energy (TKE) profiles. However, they found that the height of the TIBL can be best determined from the minimum of heat flux profiles. Hara et al. (2009) simulated the TIBL using a wind tunnel and direct numerical simulations and found that the TIBL height could be estimated from the vertical profile of the local Richardson number. Levitin and Kambezidis (1997) utilized the Boundary Layer Transformation Model (BLTM) and defined the TIBL height as the level at which the eddy diffusivity value returns to the background, or over-sea value. Moreover, the observed TIBL heights were estimated using tethered balloons and defined as the first inversion base height in the temperature profiles. The TIBL height is mainly affected by turbulence, and the turbulence properties within the TIBL can be related to three external parameters: the surface sensible heat flux over land, the onshore low-level wind speed, and the stability of the onshore airflow (Shao et al., 1991; Smedman and Högström, 1983). The TIBL grows rapidly in neutrally stratified regions and slowly in higher regions of stable stratification (Luhar et al., 1998). Levitin and Kambezidis (1997) suggested that the main input parameters that affect TIBL development are the land-sea temperature difference and wind speed. Kang et al. (2010) analyzed radiosonde data from three stations in a coastal region of Shandong Province and derived the variation in the TIBL height with inland distance, thereby yielding an empirical model of TIBL height.

The Qinhuangdao downtown area is adjacent to Bohai Bay to the east and the Yanshan Mountain chains to the west in North China. The unique geographical position results in a complicated meteorological environment. The formation of the TIBL is a common boundary layer phenomenon in the coastal region in summer. When hazardous gases are emitted into the atmosphere, the emitted gases are dispersed more horizontally than vertically in the inversion layer above the TIBL. However, once the pollutants enter the TIBL, they are dispersed both horizontally and vertically due to convective motions in the TIBL. When the pollutants reach the ground through convection, they become harmful to humans. In this paper, we first introduce the data and methods used in the study and describe the ceilometer. Second, we then analyze the differences in meteorological conditions and air pollutant characteristics between the days with and without TIBL formation. Finally, the causes of these differences are explained.

1. Data and methods

1.1. Ceilometer and the determination of the boundary layer height

This experiment adopted an enhanced single-lens LIDAR ceilometer (CL51, Vaisala, Finland). This instrument utilizes pulsed diode laser LIDAR technology to detect the profile of the atmospheric-attenuated backscattering coefficient. The ceilometer was located at the Chinese Environmental Management College in Qinhuangdao, 1.13 km away from the coastline. The longitude and latitude of the station were 39.914°N and 119.556°E, and it was settled 18 m above ground level. The main parameters of the CL 51 are presented in Table 1.

Due to the long lifetime of fine particles, ranging from several days to dozens of days, the concentration of particulate matter in the atmospheric mixing layer is much more homogeneous than those of gaseous pollutants. Moreover, a large difference exists in the particulate concentration between the atmospheric boundary layer and the free atmosphere. By analyzing the attenuated backscattering coefficient profiles of atmospheric particulates, the position where a sudden change occurs in the

Table 1 – Main parameters of the CL51 ceilometer.

Performance	Parameter
Measurement range	13 km
Reporting period	6–120 sec
Reporting precision	10 m
Peak power	27 W
Wavelength	910 nm

profile can be defined as the top of the atmospheric boundary layer. Detailed information regarding this approach has been reported in previous studies (Tang et al., 2015, 2016; Zhu et al., 2016).

1.2. Meteorological data and pollutant concentration data

The meteorological data adopted in this study were averaged each hour from June to August 2015. The TIBL is always associated with a sea breeze, so the meteorological factors used in this research included wind speed, wind direction, air temperature, relative humidity and precipitation. The meteorological data were obtained from the website of the China Meteorological Administration (http://www.weather.com.cn).

The pollutant concentration data, including PM_{10}, $PM_{2.5}$, O_3, SO_2, NO_2 and CO, which are commonly measured in China according to the Ambient Air Quality Standards (GB 3095-2012), were average values per hour over the same period. All of the pollutant concentration data were obtained from the website published by the Ministry of Environmental Protection of the People's Republic of China (http://www.zhb.gov.cn/).

2. Results and discussion

2.1. The number of days with and without a TIBL

As shown in Fig. 1, the monthly average boundary layer height in Beijing, which is an inland city, reaches the maximum value of 791 m in July. However, the monthly average boundary layer height in Qinhuangdao, which is a coastal city, displays a bimodal distribution, with a lower peak of 567 m in April and a higher peak of 603 m in August. Additionally, low values can be observed in June and July, which suggests that the TIBL causes the boundary layer height to decrease in summer.

The wind direction perpendicular to the coastline and towards the land is 157°. Therefore, wind directions between 67° and 247° are considered sea breezes, and wind directions between 0° and 67°and between 247° and 360° are considered land breezes. According to the meteorological data, the number of days with sea breezes in the daytime was 70 out of the 92 days in June, July and August 2015.

Table 2 – Summary of meteorological variables on days with (TIBL) and without (NO TIBL) a TIBL.

	T (°C)	RH (%)	BLH (m)	WS (m/sec)	SD (hr)
No-TIBL					
Average	22	79	519	1.6	7.9
Std. dev.	3.6	15.4	460.5	1.0	4.3
TIBL					
Average	22	83	311	1.4	10.3
Std. dev.	3.6	13.8	202	1.0	2.7

T: temperature; RH: relative humidity; BLH: boundary layer height; WS: wind speed; SD: sunshine duration; TIBL: thermal internal boundary layer.

If the wind blows from the sea and the boundary layer height is lower than 500 m, as indicated by the ceilometer, a TIBL forms. According to the boundary layer height data obtained by the ceilometer, the 92 days in June, July and August 2015 can be divided into three categories. The first category referred to the days without ceilometer detection; the second category referred to the days with a TIBL, and the last category referred to days without a TIBL. After screening, the number of days without ceilometer detection was 23, the number of days with a TIBL was also 23, and the number of days without a TIBL was 46.

2.2. Meteorological variables with or without a TIBL

2.2.1. Statistical characteristics of meteorological variables

Based on the meteorological data, we calculated the average and standard deviation of each meteorological variable when a TIBL formed and when no TIBL formed. As shown in Table 2, the temperature difference was small between days with and without a TIBL. However, on days with a TIBL, the relative humidity was higher than on days without a TIBL. In addition, the boundary layer height and wind speed were lower on days with a TIBL than on days without a TIBL, and the sunshine duration was 2.4 hr longer on average.

A wind angle of 157° corresponds to a SSE direction. In Fig. 2a, when there is no TIBL, the dominant wind direction is ESE. Additionally, NNE, NE and NEE winds are common, and these directions represent land breezes. In Fig. 2b, when there

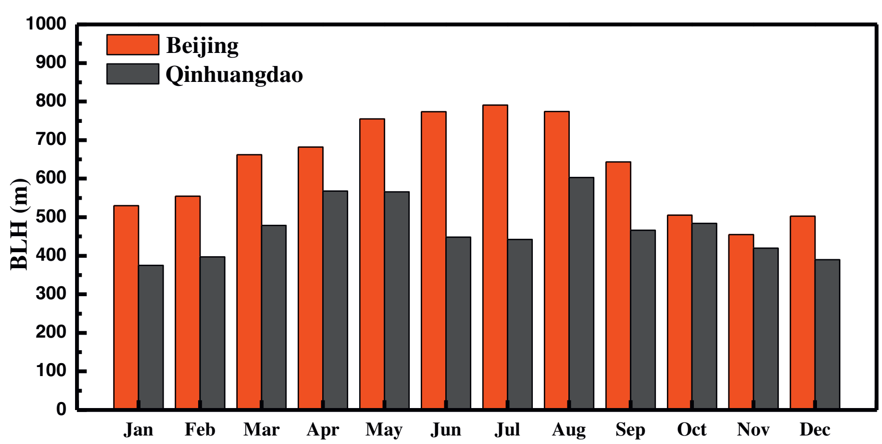

Fig. 1 – Monthly average boundary layer height (BLH) in Beijing and Qinhuangdao from September 2014 to August 2015.

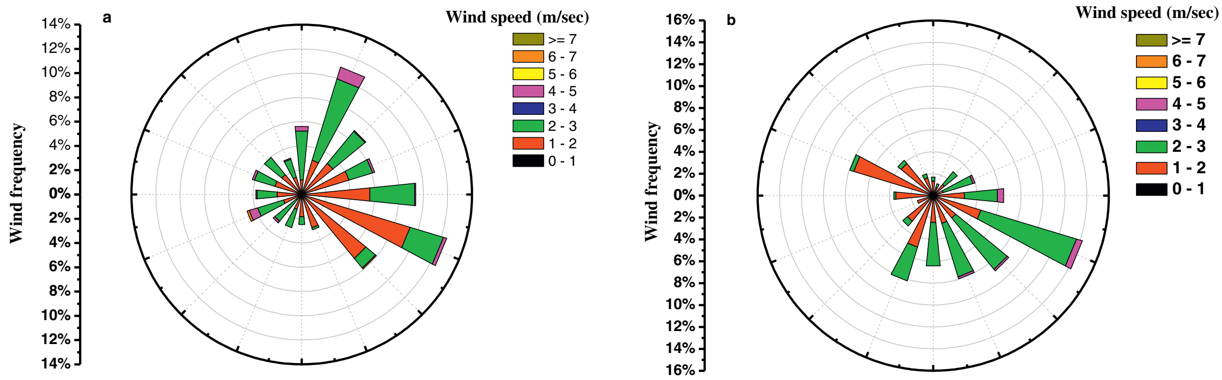

Fig. 2 – Wind frequency in Qinhuangdao in the absence (a) and presence (b) of a thermal internal boundary layer.

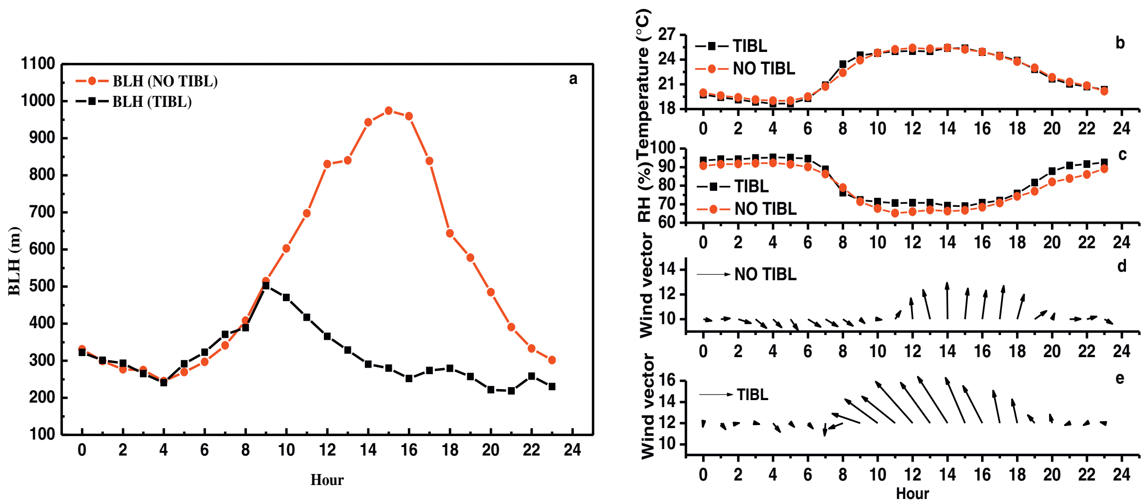

Fig. 3 – Diurnal variations in the boundary layer height (a), temperature (b), relative humidity (RH) (c) and wind vectors (d and e) in Qinhuangdao on days with and without a TIBL.

is a TIBL, the dominant wind direction is also ESE. In this case, the ESE, SE, SSE and SSW wind directions are common, and these are all sea breezes. Therefore, in Qinhuangdao in summer, the sea breezes appear more frequently on days with a TIBL than without a TIBL.

2.2.2. *Diurnal variations in meteorological variables*

After processing the ceilometer data from June, July and August 2015, the hourly average value of the boundary layer height from 0:00 LT on June 1, 2015, to 23:00 LT on August 31, 2015, was calculated. As indicated by the ceilometer data, the average value of boundary layer height in Qinhuangdao in summer was 450 ± 406 m. The occurrence frequency was highest within the 0–200 m height interval (up to 35.4%). Additionally, in this interval, a stable boundary layer was observed at night, and the TIBL was observed in the daytime.

The statistical diurnal variation in the boundary layer height on days with and without a TBL is shown in Fig. 3. On days without a TIBL, the variation is relatively regular, reaching a minimum of 245 m at 4:00 LT and a maximum of 959 m at 16:00 LT. When the TIBL is present, the average boundary layer height is relatively low, and the maximum is 502 m at approximately 9:00 LT. Consequently, due to the influence of the sea breeze, the height of the boundary layer rapidly decreases and reaches a minimum of 219 m at 21:00 LT. In addition, at 4:00 LT, the boundary layer height also reaches an extreme minimum value of 241 m.

Table 3 – Descriptive statistics of pollutant concentrations on days with (TIBL) and without (NO TIBL) a TIBL (units: CO-mg/m^3; all others-μg/m^3).

	$PM_{2.5}$	PM_{10}	CO	NO_2	O_3	O_3-8h	SO_2
NO-TIBL							
Average	29.9	74.0	1.1	34.6	53.6	82.7	13.7
Std. dev.	29.1	54.1	0.8	20.5	36.5	36.7	7.7
TIBL							
Average	29.2	73.8	0.9	33.0	55.7	84.6	11.8
Std. dev.	18.8	43.5	0.7	22.8	35.5	28.3	7.3

Note: O_3-8h represents the daily maximum value of eight-hourly averaged concentration. TIBL: thermal internal boundary layer.

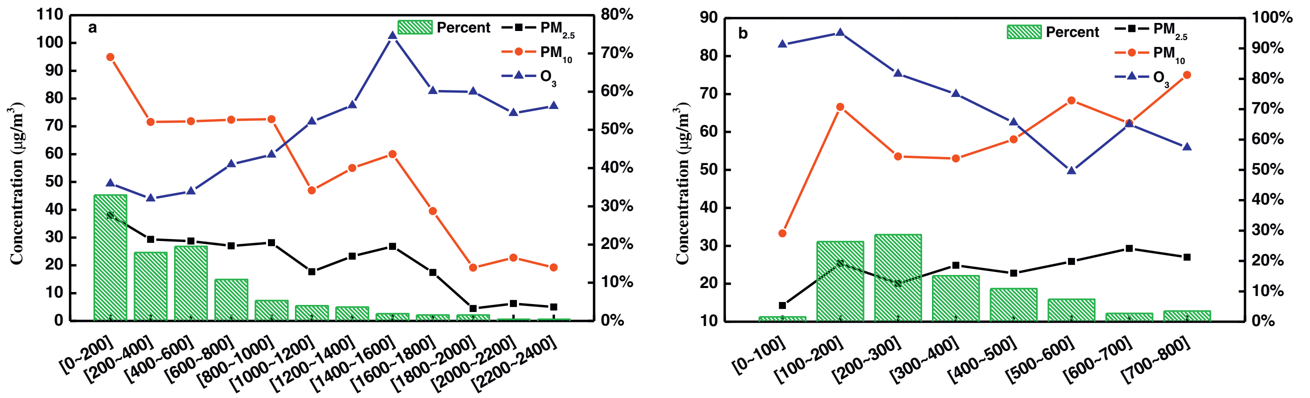

Fig. 4 – Frequency of occurrence of the boundary layer height and the variations in the average concentrations of $PM_{2.5}$, PM_{10} and O_3 with the boundary layer height on days with (a) and without (b) a TIBL. TIBL: thermal internal boundary layer.

The diurnal variation in the wind vectors is shown in Fig. 3. The wind direction perpendicular to the coastline and towards land is 157°. When there is a TIBL, the average wind speed is low from 0:00 LT to 8:00 LT and this wind is a land breeze. After 9:00 LT, the average wind is a sea breeze, and the boundary layer height reaches a maximum. From 9:00 until 18:00, a relatively strong sea breeze exists, which reaches a maximum value of 2.3 m/sec at 12:00 LT, causing the TIBL formation. Thus, the boundary layer height remains at a low level. After 18:00 LT, the average wind speed decreases rapidly. When no TIBL forms, a land breeze with a low wind speed occurs from 0:00 LT to 10:00 LT. A southerly wind occurs from 12:00 LT to 18:00 LT, with a

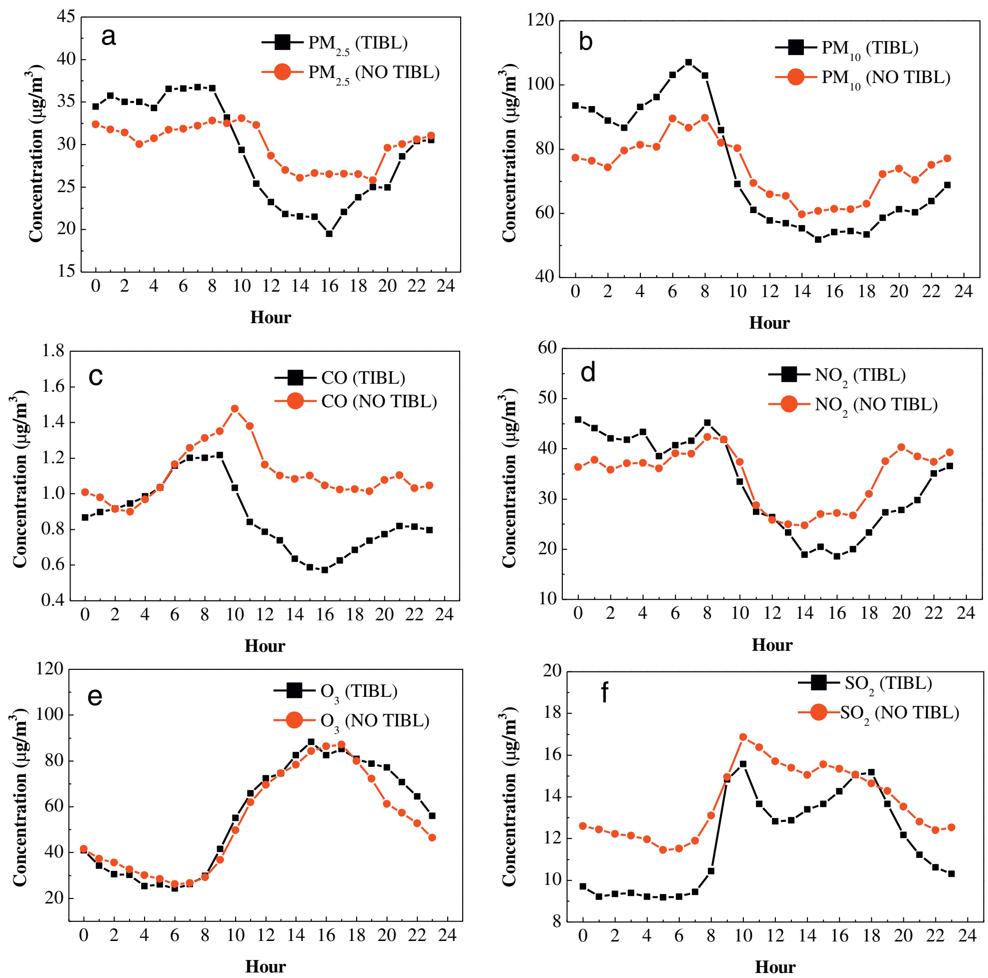

Fig. 5 – Diurnal variations in $PM_{2.5}$ (a), PM_{10} (b), CO (c), O_3 (e) and SO_2 (f) mass concentrations on days with and without a TIBL. TIBL: thermal internal boundary layer.

maximum wind speed of 1.4 m/sec at 14:00 LT. In this period, the average wind speed is much lower than when a TIBL forms. Therefore, the boundary layer height is higher in this case.

As shown in Fig. 3, the diurnal variations in temperature on days with and without a TIBL are similar, which indicates that the TIBL has little effect on the air temperature. However, the relative humidity when there is a TIBL is slightly higher than when there is no TIBL, because the air from the sea is damper than that from the land.

2.3. Influence of the TIBL on pollutant concentrations

2.3.1. Statistical characteristics of pollutant concentrations

As shown in Table 3, when a TIBL forms, the average concentrations of $PM_{2.5}$ and PM_{10} are nearly as high as when there is no TIBL, and the average concentrations of CO, NO_2 and SO_2 are lower than when no TIBL forms. Additionally, the average concentrations of O_3 and O_3-8h are both higher on days with a TIBL compared to days without a TIBL.

2.3.2. Variations in air pollutants on days with and without a TIBL

After separating the data from days with and without a TIBL, we can calculate the average concentrations of pollutants in each height interval.

As shown in Fig. 4a, when there is no TIBL, the average concentrations of $PM_{2.5}$ and PM_{10} at each height interval decrease with increasing height. Since the boundary layer height is an important physical quantity that influences the vertical diffusion of pollutants, pollutants cannot easily diffuse if compressed within the mixing layer when the boundary layer height is low. This process will lead to high pollutant concentrations. If the boundary layer height is relatively high, pollutants will have low concentrations due to dilution within the boundary layer. However, the concentration of O_3 increases with the boundary layer height because a high boundary layer height accompanied by strong solar radiation is favorable for the production of O_3 under the effects of photochemical reactions.

When a TIBL forms, the average concentrations of $PM_{2.5}$ and PM_{10} increase in each height interval and the concentration of O_3 decreases with increasing boundary layer height, as shown in Fig. 4b. These observations occur because the boundary layer height is mainly between 100 and 300 m on days with a TIBL, and this height is generally associated with a strong sea breeze. Because of the dilution effect of the sea breeze, the concentration of particulate matter is low in this height interval. In addition, solar radiation is strong when a TIBL forms, which is favorable for the production of O_3. Therefore, the concentration of O_3 is high in the height intervals from 100 m to 300 m. In the height intervals from 700 m to 800 m, the concentrations of particulate matter and O_3 are approximately equal on days with and without TIBLs, which suggests that the effect of the TIBL on pollutants is not obvious in this height interval.

After separating the days with and without TIBLs, the diurnal variations in air pollutant concentrations could be determined, and the influence of the TIBL on air pollutants was investigated. In the coastal region in summer, the daytime sea breeze is a common synoptic phenomenon. When the sea breeze is present, the concentrations of air pollutants are generally lower due to dilution effects.

As shown in Fig. 5, at 9:00 LT in the morning, the concentrations of both $PM_{2.5}$ and PM_{10} decrease due to the dilution effects of the sea breeze and reach minimum levels until 16:00 LT on days with and without a TIBL. After 16:00 LT, due to

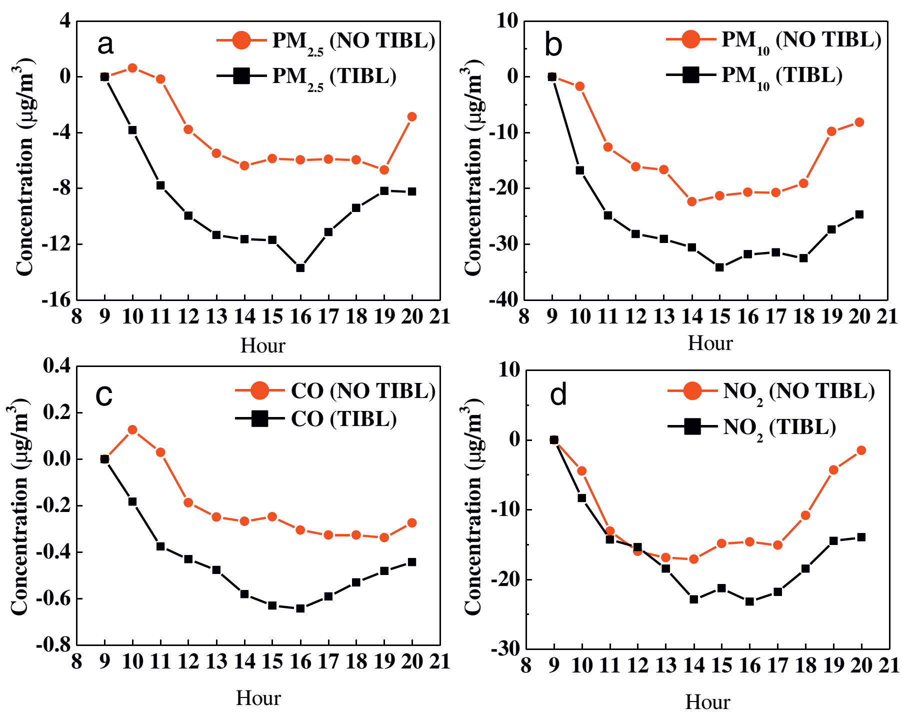

Fig. 6 – Diurnal variations in the hourly mass concentrations of $PM_{2.5}$ (a), PM_{10} (b), CO (c) and NO_2 (d) from 9:00 LT to 20:00 LT minus their mass concentration at 9:00 LT on days with and without a TIBL. TIBL: thermal internal boundary layer.

Table 4 – Maximum, minimum values and daily ranges of air pollutants concentrations on days with (TIBL) and without (NO TIBL) a TIBL (unit: CO-mg/m^3; all others-μg/m^3).

	$PM_{2.5}$	PM_{10}	CO	NO_2	O_3	SO_2
NO-TIBL						
Maximum	33.1	89.7	1.48	42.4	87.2	16.8
Minimum	25.8	59.6	0.9	24.7	26.2	11.5
Max–Min	7.3	30.1	0.58	17.7	61.0	5.3
TIBL						
Maximum	36.7	107.1	1.22	45.8	88.2	15.6
Minimum	19.5	51.8	0.67	18.6	24.3	9.2
Max–Min	17.2	55.3	0.65	27.2	63.9	6.4

TIBL: thermal internal boundary layer.

the weakening of the sea breeze, the concentrations of both $PM_{2.5}$ and PM_{10} increase. However, as shown in Fig. 6, the increases in $PM_{2.5}$ and PM_{10} concentrations on days with a TIBL are faster than on days without a TIBL. This finding implies that the TIBL causes air pollutants to accumulate at a rapid rate.

Additionally, the diurnal variations in CO are similar to those in $PM_{2.5}$ and PM_{10}. However, the diurnal variation in O_3 differs. Comparing the days with and without a TIBL, the diurnal variations in the average concentration of O_3 are nearly the same, as shown in Fig. 5e. This result suggests that local photochemical reactions are the main source of boundary layer O_3 in the daytime. Because NO_2 is a precursor of O_3, the concentrations of the two are often negatively correlated, as shown in Fig. 5d and e.

The oxidation of VOCs (Volatile organic compounds) is a major source of CO, so variations in VOCs can be replaced with variations in CO. In addition, due to the high concentration of O_3 in summer, NO_2 accounts for a large proportion of NO_x. In Fig. 5c, d, the concentration of CO increases by 82% at 16:00 LT on days with a TIBL compared to days without a TIBL, and the concentration of NO_2 simultaneously increases by 47%. Moreover, in Fig. 5e the concentration of O_3 does not vary much on days with *vs.* those without a TIBL. Therefore, it can be inferred that the production of O_3 is sensitive to VOCs in summer in Qinhuangdao, which was also noted in previous studies (Tang et al., 2012, 2017b).

The diurnal variations in CO and SO_2 display bimodal distributions. For CO, a high peak of 1.22 mg/m^3 at 9:00 LT and a low peak of 0.82 mg/m^3 at 21:00 LT occur on days with a TIBL. For SO_2, a high peak of 15.6 μg/m^3 at 10:00 LT and a low peak of 15.2 μg/m^3 at 18:00 LT occur on days with a TIBL. These peaks are likely due to fossil fuel combustion.

As shown in Table 4, except for the maximum values of CO and SO_2, the maximum concentrations of air pollutants are larger and minimum concentrations are smaller when there is a TIBL compared to when no TIBL forms. Therefore, the diurnal ranges of all air pollutants are larger than when there is no TIBL. This result implies that the TIBL worsens air pollution at the daily scale.

3. Conclusions

In this study, we used a ceilometer to determine the boundary layer height at a coastal site in Qinhuangdao. Using meteorological data, we found that a TIBL formed on 23 days, while no TIBL was observed on 46 days and ceilometer data were unavailable on 23 days in June, July and August 2015.

In summer, the average temperature was the same on days with and without TIBLs, and the dominant wind was a sea breeze. The relative humidity was higher and the sunshine duration was 2.4 hr longer on days with a TIBL compared to days without a TIBL. The TIBL caused the boundary layer height to decrease considerably after 9:00 LT at the daily scale. This relationship is associated with the wind speed, which is higher on days with a TIBL.

As the boundary layer rose on days without a TIBL, the average concentrations of particulate matter decreased and the average concentration of O_3 increased due to diffusion and photochemical reactions, respectively. However, the average concentrations of particulate matter increased and the average concentration of O_3 decreased with increasing boundary layer height on days with TIBLs. Notably, in the height interval from 100 m to 300 m, in which the TIBL height typically falls, the concentrations of particulate matter are low due to the dilution effects of the sea breeze. Under such conditions, strong solar radiation is favorable for the production of O_3.

Due to the dilution effects of the sea breeze, the concentrations of $PM_{2.5}$ and PM_{10} reached minimums at 16:00 LT. Subsequently, the $PM_{2.5}$ and PM_{10} concentrations increased at faster rates on days with a TIBL compared to days without a TIBL, which implies that the TIBL causes air pollutants to accumulate rapidly. However, the diurnal variation in O_3 concentration was similar on all days, because local photochemical reactions are the main source of boundary layer O_3 in the daytime. Based on the diurnal variations in CO, NO_2 and O_3, it can be inferred that the production of O_3 is sensitive to VOCs in summer in Qinhuangdao.

The diurnal variations in CO and SO_2 exhibited bimodal distributions, and the diurnal variations in other air pollutants displayed single peak distributions. Excluding the maximum values of CO and SO_2, the maximum concentrations of air pollutants on days with a TIBL were larger than those on days without a TIBL. Because of the low concentrations of air pollutants and long sunshine duration, it is suitable for the citizens to do outdoor activities in the daytime on days with a TIBL. These results can be applied to control strategies of air pollutants on days with a TIBL during summer in Qinhuangdao and similar coastal cities in North China.

Acknowledgments

This work was supported by the National Key R&D Program of China (No. 2017YFC 0210000), the National Natural Science Foundation of China (Nos. 41230642 and 41705113), and the Beijing Municipal Science and Technology Project (No. ZL171100000617002).

REFERENCES

Beyrich, F., 1997. Mixing height estimation from sodar data — a critical discussion. Atmos. Environ. 31, 3941–3953.

Calmet, I., Mestayer, P., 2016. Study of the thermal internal boundary layer during sea-breeze events in the complex coastal area of Marseille. Theor. Appl. Climatol. 123, 801–826.

Emeis, S., Schäfer, K., 2006. Remote sensing methods to investigate boundary-layer structures relevant to air pollution in cities. Bound.-Layer Meteorol. 121, 377–385.
Emeis, S., Schäfer, K., Münkel, C., 2008. Surface-based remote sensing of the mixing-layer height - a review. Meteorol. Z. 17, 621–630.
Garratt, J.R., 1990. The internal boundary layer — a review. Bound.-Layer Meteorol. 50, 171–203.
Hara, T., Ohya, Y., Uchida, T., Ohba, R., 2009. Wind-tunnel and numerical simulations of the coastal thermal internal boundary layer. Bound.-Layer Meteorol. 130, 365–381.
Kang, L., Cai, X., Zhang, H., Zhang, M., Wang, Z., Chen, J., 2010. Thermal internal boundary layer over Shidaowan nuclear power station site, Shandong Province. Radiat. Prot. 30, 65–69.
Levitin, J., Kambezidis, H.D., 1997. Numerical modelling of the thermal internal boundary-layer evolution using ATHENS field experimental data. Bound.-Layer Meteorol. 84, 207–217.
Luhar, A.K., Sawford, B.L., Hacker, J.M., Rayner, K.N., 1998. The Kwinana coastal fumigation study: ii — growth of the thermal internal boundary layer. Bound.-Layer Meteorol. 89, 385–405.
Prabha, T.V., Venkatesan, R., Mursch-Radlgruber, E., Rengarajan, G., Jayanthi, N., 2002. Thermal internal boundary layer characteristics at a tropical coastal site as observed by a mini-SODAR under varying synoptic conditions. J. Earth Syst. Sci. 111, 63–77.
Scarino, A.J., Obland, M.D., Fast, J.D., Burton, S.P., Ferrare, R.A., Hostetler, C.A., et al., 2014. Comparison of mixed layer heights from airborne high spectral resolution lidar, ground-based measurements, and the WRF-Chem model during CalNex and CARES. Atmos. Chem. Phys. 14, 5547–5560.
Seibert, P., Beyrich, F., Gryning, S.E., Joffre, S., Rasmussen, A., Tercier, P., 2000. Review and intercomparison of operational methods for the determination of the mixing height. Atmos. Environ. 34, 1001–1027.
Shao, Y., Hacker, J.M., Schwerdtfeger, P., 1991. The structure of turbulence in a coastal atmospheric boundary layer. Q. J. R. Meteorol. Soc. 117, 1299–1324.
Sicard, M., Pérez, C., Rocadenbosch, F., Baldasano, J.M., García-Vizcaino, D., 2006. Mixed-layer depth determination in the Barcelona coastal area from regular lidar measurements: methods, results and limitations. Bound.-Layer Meteorol. 119, 135–157.
Smedman, A.S., Högström, U., 1983. Turbulent characteristics of a shallow convective internal boundary layer. Bound.-Layer Meteorol. 25, 271–287.
Stull, R.B., 1988. An Introduction to Boundary Layer Meteorology. Kluwer Academic Publishers.
Tang, G., Wang, Y., Li, X., Ji, D., Hsu, S., Gao, X., 2012. Spatial-temporal variations in surface ozone in Northern China as observed during 2009-2010 and possible implications for future air quality control strategies. Atmos. Chem. Phys. 12, 2757–2776.
Tang, G., Zhu, X., Hu, B., Xin, J., Wang, L., Münkel, C., et al., 2015. Impact of emission controls on air quality in Beijing during APEC 2014: lidar ceilometer observations. Atmos. Chem. Phys. 15, 12667–12680.
Tang, G., Zhang, J., Zhu, X., Song, T., Münkel, C., Hu, B., et al., 2016. Mixing layer height and its implications for air pollution over Beijing, China. Atmos. Chem. Phys. 16, 2459–2475.
Tang, G., Zhao, P., Wang, Y., Gao, W., Cheng, M., Xin, J., Li, X., Wang, Y., 2017a. Mortality and air pollution in Beijing: the long-term relationship. Atmos. Environ. 150, 238–243.
Tang, G., Zhu, X., Xin, J., Hu, B., Song, T., Sun, Y., et al., 2017b. Modelling study of boundary-layer ozone over northern China — part I: ozone budget in summer. Atmos. Res. 187, 128–137.
White, A.B., Senff, C.J., Banta, R.M., 2010. A comparison of mixing depths observed by ground-based wind profilers and an airborne lidar. J. Atmos. Ocean. Technol. 16, 584–590.
Wiegner, M., Emeis, S., Freudenthaler, V., Heese, B., Junkermann, W., Muenkel, C., et al., 2006. Mixing layer height over Munich, Germany: variability and comparisons of different methodologies. J. Geophys. Res.-Atmos. 111.
Zhu, X., Tang, G., Hu, B., Wang, L., Xin, J., Zhang, J., et al., 2016. Regional pollution and its formation mechanism over North China Plain: a case study with ceilometer observations and model simulations. J. Geophys. Res.-Atmos. 121, 14574–14588.